Thermodynamic meaning of local temperature of nonequilibrium open quantum systems

LvZhou Ye,[1] Xiao Zheng,[1,2,*] YiJing Yan,[1,3] and Massimiliano Di Ventra[4,†]

[1]*Hefei National Laboratory for Physical Sciences at the Microscale, University of Science and Technology of China, Hefei, Anhui 230026, China*

[2]*Synergetic Innovation Center of Quantum Information and Quantum Physics, CAS Center for Excellence in Nanoscience, University of Science and Technology of China, Hefei, Anhui 230026, China*

[3]*iChEM (Collaborative Innovation Center of Chemistry for Energy Materials), University of Science and Technology of China, Hefei, Anhui 230026, China*

[4]*Department of Physics, University of California, San Diego, La Jolla, California 92093, USA*

(Received 22 August 2016; revised manuscript received 15 October 2016; published 2 December 2016)

Measuring the local temperature of nanoscale systems out of equilibrium has emerged as a new tool to study local heating effects and other local thermal properties of systems driven by external fields. Although various experimental protocols and theoretical definitions have been proposed to determine the local temperature, the thermodynamic meaning of the measured or defined quantities remains unclear. By performing analytical and numerical analysis of bias-driven quantum dot systems both in the noninteracting and strongly-correlated regimes, we elucidate the underlying physical meaning of local temperature as determined by two definitions: the zero-current condition that is widely used but not measurable and the minimal-perturbation condition that is experimentally realizable. We show that, unlike the zero-current condition, the local temperature determined by the minimal-perturbation protocol establishes a quantitative correspondence between the nonequilibrium system of interest and a reference *equilibrium* system, provided the probed system observable and the related electronic excitations are fully local. The quantitative correspondence thus allows the well-established thermodynamic concept to be extended to nonequilibrium situations.

DOI: 10.1103/PhysRevB.94.245105

I. INTRODUCTION

Probing the variation of local temperatures in systems out of equilibrium has become a subject of intense experimental interest in physics [1–5], chemistry [6–8], and life sciences [9–12]. With the development of high-resolution thermometry techniques, measurement of some sort of temperature distributions of nonequilibrium systems has been realized, such as in graphene-metal contacts [4], gold interconnect structures [5], and living cells [12].

Local electronic and phononic excitations occur in nanoelectronic devices subject to a bias voltage or thermal gradient, and hence the devices are supposedly at a local temperature somewhat higher than the background temperature. Such local heating affects crucially the device properties [13–16] and has significant influence on some physical processes, such as thermoelectric conversion [17–19], heat dissipation [8,19], and electron-phonon interactions [20,21]. All these studies, however, leave open the question of what precisely is a "local temperature" in a nonequilibrium system, a concept that has a well-established meaning only in global equilibrium.

Over the past decade, numerous experimental [15,22–28] and theoretical [29–41] efforts have been made to provide practical and meaningful definitions of local temperature for nonequilibrium systems that bear a close conceptual resemblance to the thermodynamic one. However, it has remained largely unclear how to physically interpret the defined local temperature and how to associate the measured value with the magnitudes of local excitations at a quantitative level.

This work aims at elucidating these fundamental issues through analytical and numerical analysis on nonequilibrium quantum dot (QD) systems. In particular, we shall focus on the definition of local temperature based on the zero-current condition proposed by Engquist and Anderson [42] and that based on the minimal-perturbation condition as proposed in Refs. [32,39]. To enable an analytical analysis and quantitatively accurate numerical studies, in this work we shall concentrate on the low-background-temperature regime, so that the local excitations on a QD are dominated by the scattering events and correlation effects among electrons, while phonon modes are not promoted.

The remainder of this paper is organized as follows. In Sec. II the model and methodology used in this work is introduced. In Sec. III we present analytical analysis on local temperatures of bias-driven QD systems. A quantitative correspondence relation is proposed. In Sec. IV, numerical calculation results are given for QDs in both noninteracting and strongly-correlated regimes. The physical meaning of local temperatures is further elaborated. Concluding remarks are given in Sec. V.

II. METHODOLOGY AND MODEL

A. Zero-current condition

The definition of local temperature based on the zero-current condition (ZCC) has been used extensively in the literature [31,34,36,37,43–47]. The basic idea is to couple an ideal potentiometer/thermometer (the probe) to the nonequilibrium system of interest. By varying the temperature (T_p) and

*xz58@ustc.edu.cn
†diventra@physics.ucsd.edu

chemical potential (μ_p) of the probe until the electric current (I_p) and heat current ($J_p^{\rm H}$) flowing through the probe both vanish, the local temperature (T^*) and local chemical potential (μ^*) of the system are determined as $T^* = T_p$ and $\mu^* = \mu_p$, respectively. In short, the ZCC is expressed as (hereafter we set $e = \hbar = k_{\rm B} = 1$)

$$I_p(T_p = T^*, \mu_p = \mu^*) = 0, \tag{1a}$$

$$J_p^{\rm H}(T_p = T^*, \mu_p = \mu^*) = 0. \tag{1b}$$

The ZCC is often referred to as the "local equilibrium condition," as the determined local temperature can be understood from the perspective of the zeroth law of thermodynamics. However, such a *macroscopic* definition of local temperature does not reflect the *microscopic* change of the system state in a nonequilibrium situation. Moreover, it is important to note that, unlike charge currents, we have no means to *directly* measure heat currents, since in the latter case we have no equivalent apparatus like the ammeter in the electronic case [16]. This is an often ignored but very important issue that severely limits the experimental application of the ZCC-based definition.

B. Minimal-perturbation condition

The minimal-perturbation condition (MPC) based definition is conceptually different. Consider an open quantum system whose dynamics is described by a quantum master equation for the system reduced density matrix ρ

$$\dot{\rho}(t) = -i[H_{\rm sys}, \rho] + \mathcal{R}_{\rm env}[\rho], \tag{2}$$

where $H_{\rm sys}$ is the system Hamiltonian, and $\mathcal{R}_{\rm env}[\rho]$ is a superoperator that represents the dissipative interactions between the system and its environment. As initially proposed by Dubi and Di Ventra [32,33], to determine the local temperature of the system (T^*), one could couple an external probe to the system. This would introduce an additional dissipation term $\mathcal{R}_p[\rho]$ on the right-hand side of Eq. (2), which accounts for the system-probe interactions. T^* is determined by tuning the temperature of the probe (T_p) so that the coupling probe has minimal perturbation to the system dynamics (the additional dissipation term $\mathcal{R}_p[\rho]$ gets minimized). The T^* determined in this way then reflects directly the change of system states.

While in principle the MPC should be imposed on ρ that directly reflects the change of system states, in practice it is difficult to monitor the evolution of ρ in experiments. Therefore, for practical purpose, we choose to impose the MPC on the expectation value of a certain system observable $O = \langle \hat{O} \rangle = {\rm tr}(\rho \hat{O})$ [39].

Consider, for instance, a QD connected to two leads (L and R), with the lead temperatures (chemical potentials) being T_L and T_R (μ_L and μ_R), respectively. By locally coupling a probe to the QD, the expectation value of a local observable $O = \langle \hat{O} \rangle$ is subjected to a perturbation, $\delta O_p(T_p, \mu_p)$, which depends explicitly on T_p and μ_p.

An experimentally feasible way to determine T^* and μ^* is to vary μ_p and T_p, until the electric current through the probe vanishes and simultaneously the perturbation $\delta O_p(T_p, \mu_p)$ gets minimized [32,39]:

$$I_p(T_p = T^*, \mu_p = \mu^*) = 0, \tag{3a}$$

$$T^* = \arg\min_{T_p} |\delta O_p(T_p, \mu_p)|. \tag{3b}$$

As is evident, the use of Eqs. (3a) and (3b) does not require the measurement of heat currents.

Theoretically it is rather difficult to find analytical solutions for μ^* and T^* through Eqs. (3a) and (3b), since they usually lead to coupled nonlinear equations. For simplicity, and also for a more transparent physical understanding, we adopt a two-step approach to determine T^* and μ^*—we first determine μ^* as a weighted sum of μ_L and μ_R [see Eq. (4) below], and then T^* is determined by imposing the MPC of Eq. (3b). As will be shown later in Sec. III A, the approximation made for μ^* does not alter the conclusions and understanding reached through this work.

For a QD subjected to a bias voltage $V = \mu_R - \mu_L$, the local chemical potential μ^* is first determined as [39]

$$\mu^* = \zeta_L \mu_L + \zeta_R \mu_R. \tag{4}$$

Then the local temperature T^* is measured by varying T_p, with μ_p fixed at the value determined by Eq. (4)

$$\delta O_p(T_p, \mu_p) = \zeta_L O_p(T_L, \mu_L) + \zeta_R O_p(T_R, \mu_R) - O_p(T_p, \mu_p). \tag{5}$$

Here, $O_p(T_\alpha, \mu_\alpha)$ denotes the local observable $\langle \hat{O} \rangle$ measured by setting $T_p = T_\alpha$ and $\mu_p = \mu_\alpha$ ($\alpha = L$ or R), and the weight coefficients ζ_L and ζ_R are determined by

$$\zeta_\alpha = 1 - \left| \frac{I_p(T_\alpha, \mu_\alpha)}{I_p(T_L, \mu_L) - I_p(T_R, \mu_R)} \right|. \tag{6}$$

It has been verified in Ref. [39] that Eq. (4) is a reasonable and convenient approximation for μ^*.

At zero bias T^* determined by Eq. (3b) recovers exactly the physical equilibrium temperature. While in many cases the MPC-defined T^* is numerically close to that obtained by the ZCC [39], the former does not require the measurement of heat currents, and hence its experimental realization is feasible. Despite this added benefit, it remains unclear how T^* determined by Eq. (3b) is quantitatively related to the electronic excitations in a nonequilibrium system and what is the underlying origin of the difference between the ZCC and MPC based definitions. This leads us to question to what extent can we assign to the MPC quantity the meaning of a "thermodynamic temperature" as in the equilibrium case.

C. Quantum impurity model for quantum dots

To address the above fundamental issues, we carry out analytical and numerical analysis on QD systems described by the single-impurity Anderson model (SIAM) [48]. The total Hamiltonian is $\hat{H} = \hat{H}_{\rm dot} + \hat{H}_{\rm lead} + \hat{H}_{\rm coup}$. The dot is represented by $\hat{H}_{\rm dot} = \epsilon_d \hat{n}_d + U \hat{n}_\uparrow \hat{n}_\downarrow$, with $\hat{n}_d = \sum_s \hat{n}_s = \sum_s \hat{a}_s^\dagger \hat{a}_s$. Here, $\hat{a}_s^\dagger$ ($\hat{a}_s$) creates (annihilates) an electron of spin s on the dot level of energy ϵ_d, and U is the on-dot electron-electron (e-e) Coulomb interaction energy. $\hat{H}_{\rm lead} = \sum_{\alpha k s} \epsilon_{\alpha k} \hat{d}_{\alpha k s}^\dagger \hat{d}_{\alpha k s}$ represents the noninteracting leads,

and $\hat{H}_{\rm coup}=\sum_{\alpha k s}(t_{\alpha k}\,\hat{a}_s^\dagger\,\hat{d}_{\alpha k s}+{\rm H.c.})$ describes the dot-lead couplings, respectively. Here, $\hat{d}^\dagger_{\alpha k s}$ ($\hat{d}_{\alpha k s}$) creates (annihilates) a spin-s electron on the state $|k\rangle$ of lead α ($\alpha=L,R$ or p), and $t_{\alpha k}$ is the coupling strength between the dot level and lead orbital $|k\rangle$. The influence of noninteracting leads can be captured by the hybridization functions $\Gamma_\alpha(\omega)\equiv\pi\sum_k|t_{\alpha k}|^2\delta(\epsilon-\epsilon_{\alpha k})$. For numerical convenience, a Lorentzian form of $\Gamma_\alpha(\omega)=\Delta_\alpha W_\alpha^2/[(\omega-\Omega_\alpha)^2+W_\alpha^2]$ is adopted, where Δ_α is the effective dot-lead coupling strength, and Ω_α and W_α are the band center and width of lead α, respectively.

As for the local observable $\hat{O}$ that is necessary for the experimental utilization of MPC, we examine two choices—the local magnetic susceptibility $\chi^m\equiv\frac{\partial\langle\hat{m}_z\rangle}{\partial H_z}|_{H_z\to0}$ and the local charge susceptibility $\chi^c\equiv-\frac{\partial\langle\hat{n}_d\rangle}{\partial\epsilon_d}$. Here, $\hat{m}_z=g\mu_{\rm B}(\hat{n}_\uparrow-\hat{n}_\downarrow)/2$ is the dot magnetization operator, with H_z being the magnetic field, g the gyromagnetic ratio, and $\mu_{\rm B}$ the Bohr magneton.

III. THERMODYNAMIC MEANING OF LOCAL TEMPERATURE AND CORRESPONDENCE RELATION

A. Analytical analysis on a single-level QD

Consider a single-level QD in a stationary state; its retarded/advanced single-electron Green's function of spin s is [49]

$$G_s^r(\omega)=\big[G_s^a(\omega)\big]^\dagger=\frac{1}{\omega-\epsilon_d-\Sigma_s^r(\omega)}. \tag{7}$$

Here, $\Sigma_s^r(\omega)=\Sigma_{\rm res}^r(\omega)+\Sigma_{\rm ee}^r(\omega)$ is the retarded self-energy, and $\Sigma_{\rm res}^r(\omega)$ and $\Sigma_{\rm ee}^r(\omega)$ arise from the dot-lead couplings and the electron-electron interactions, respectively. The lesser Green's function of the dot is $G_s^<(\omega)=G_s^r(\omega)\,\Sigma_s^<(\omega)\,G_s^a(\omega)$, with the lesser self-energy $\Sigma_s^<(\omega)=\Sigma_{\rm res}^<(\omega)+\Sigma_{\rm ee}^<(\omega)$ [49,50].

The spectral density function of the dot is $A_s(\omega)\equiv\frac{1}{2\pi}\int dt\,e^{i\omega t}\langle\{\hat{a}_s(t),\hat{a}_s^\dagger(0)\}\rangle=-\frac{1}{\pi}{\rm Im}[G_s^r(\omega)]$ and $A(\omega)=\sum_s A_s(\omega)$. The energy distribution of electric and heat currents flowing into lead α is [51,52]

$$j_{\alpha s}^k(\omega)=(-1)^{k+1}\frac{i}{\pi}(\omega-\mu_\alpha)^k\,\Gamma_\alpha(\omega)\times\big\{G_s^<(\omega)+2if_{T_\alpha,\mu_\alpha}(\omega){\rm Im}\big[G_s^r(\omega)\big]\big\}. \tag{8}$$

Here, $k=0$ and 1 correspond to the electric and heat currents, respectively, and $f_{T_\alpha,\mu_\alpha}(\omega)=1/[e^{(\omega-\mu_\alpha)/T_\alpha}+1]$ is the Fermi function. The total electric and heat currents flowing into lead α are obtained by integrating $j_{\alpha s}^k(\omega)$ over the entire energy range as $I_\alpha=\sum_s\int d\omega\,j_{\alpha s}^0(\omega)$ and $J_\alpha^{\rm H}=\sum_s\int d\omega\,j_{\alpha s}^1(\omega)$.

B. Noninteracting dots

For noninteracting dots ($U=0$), the e-e interacting self-energies [$\Sigma_{\rm ee}^r(\omega)$ and $\Sigma_{\rm ee}^<(\omega)$] vanish. For simplicity, consider all leads have the same bandwidth $W_\alpha=W$ ($\alpha=L,R$ and p), and the band centers are set to lead chemical potentials. The lead hybridization functions are

$$\Gamma_\alpha(\omega)=\frac{\Delta_\alpha W^2}{(\omega-\mu_\alpha)^2+W^2}=\Delta_\alpha\eta_\alpha(\omega). \tag{9}$$

Here, $\eta_\alpha(\omega)$ is proportional to the density of states of lead α. The electric current is expressed as

$$I_\alpha=2\int d\omega\,\Gamma_\alpha(\omega)A(\omega)\times\left\{\frac{\sum_{\alpha'}\Gamma_{\alpha'}(\omega)f_{T_{\alpha'},\mu_{\alpha'}}(\omega)}{\sum_{\alpha'}\Gamma_{\alpha'}(\omega)}-f_{T_\alpha,\mu_\alpha}(\omega)\right\}. \tag{10}$$

At $\Delta_p=0$, we have $A(\omega)=A_0(\omega)$, with $A_0(\omega)$ being the dot spectral function in the absence of the probe.

By setting $T_p=T_\alpha$ and $\mu_p=\mu_\alpha$ ($\alpha=L$ or R), respectively, it is straightforward to see that

$$\left.\frac{I_p(T_L,\mu_L)}{I_p(T_R,\mu_R)}\right|_{\Delta_p\to0}=-\frac{\Delta_R}{\Delta_L}. \tag{11}$$

The weight coefficients $\{\zeta_\alpha\}$ in Eq. (6) are determined as

$$\zeta_L=\frac{\Delta_L}{\Delta_L+\Delta_R}\quad\text{and}\quad\zeta_R=\frac{\Delta_R}{\Delta_L+\Delta_R}. \tag{12}$$

Therefore, the local chemical potential is [cf. Eq. (4)]

$$\mu^*=\frac{\Delta_L}{\Delta_L+\Delta_R}\mu_L+\frac{\Delta_R}{\Delta_L+\Delta_R}\mu_R. \tag{13}$$

The expectation values of local observables $O=\chi^c$ and χ^m can be expressed as

$$O=\mathcal{C}_O'\sum_\alpha\int d\omega\,\frac{\Gamma_\alpha(\omega)}{\sum_{\alpha'}\Gamma_{\alpha'}(\omega)}\frac{\partial A(\omega)}{\partial\epsilon_d}f_{T_\alpha,\mu_\alpha}(\omega). \tag{14}$$

Here, $\mathcal{C}_O'$ is a constant prefactor dependent on the specific choice of O.

Denote $O_0(T_L,\mu_L,T_R,\mu_R)$ as the expectation value of $\hat{O}$ in the *absence* of the probe, and its deviation from the equilibrium value is

$$\begin{aligned}&O_0(T_L,\mu_L,T_R,\mu_R)-O_0(T_{\rm eq},\mu_{\rm eq},T_{\rm eq},\mu_{\rm eq})\\&=\mathcal{C}_O'\int d\omega\left\{\frac{\Gamma_L(\omega)f_{T_L,\mu_L}(\omega)+\Gamma_R(\omega)f_{T_R,\mu_R}(\omega)}{\Gamma_L(\omega)+\Gamma_R(\omega)}\frac{\partial A_0(\omega)}{\partial\epsilon_d}\right.\\&\quad\left.-f_{T_{\rm eq},\mu_{\rm eq}}(\omega)\frac{\partial A_0(\omega)}{\partial\epsilon_d}\bigg|_{T_\alpha=T_{\rm eq},\,\mu_\alpha=\mu_{\rm eq}}\right\}.\end{aligned} \tag{15}$$

Here, $T_{\rm eq}$ and $\mu_{\rm eq}$ are the temperature and chemical potential of the QD at equilibrium, respectively.

1. The case of wide-band limit

In the wide-band limit ($W\to\infty$), the dot spectral function

$$A_s(\omega)=\frac{1}{\pi}\frac{\sum_\alpha\Delta_\alpha}{(\omega-\epsilon_d)^2+\big(\sum_\alpha\Delta_\alpha\big)^2} \tag{16}$$

is independent of μ_α and T_α. Consequently, the equilibrium and nonequilibrium dots have identical spectral functions, i.e., $A_0(\omega;\mu_L,\mu_R)=A_0(\omega;\mu_{\rm eq},\mu_{\rm eq})=A_0(\omega)$. The expectation values of local observables $O=\chi^c$ and χ^m can be expressed in a compact form of

$$O=\mathcal{C}_O\sum_\alpha\Delta_\alpha\int d\omega\,\frac{\partial A(\omega)}{\partial\epsilon_d}f_{T_\alpha,\mu_\alpha}(\omega), \tag{17}$$

with $\mathcal{C}_O=\mathcal{C}_O'/\sum_\alpha\Delta_\alpha$. The perturbation of local observable O by the coupled probe assumes the following general form

[cf. Eq. (5)]:

$$\delta O_p(T_p,\mu_p) = -\mathcal{C}_O\,\Delta_p \int d\omega\,\frac{\partial A(\omega)}{\partial \epsilon_d}\left\{ f_{T_p,\mu_p}(\omega) - \frac{\Delta_L f_{T_L,\mu_L}(\omega) + \Delta_R f_{T_R,\mu_R}(\omega)}{\Delta_L+\Delta_R}\right\}. \quad (18)$$

Apparently, imposing the MPC on χ^m or χ^c would lead to exactly the same T^*, since the right-hand side of Eq. (18) differs only in the constant prefactor $\mathcal{C}_O$ for different choice of O.

Let us now examine in detail how the excitations induced by a bias voltage or thermal gradient affect the local observable O. Equation (15) now reduces to

$$O_0(T_L,\mu_L,T_R,\mu_R) - O_0(T_{\rm eq},\mu_{\rm eq},T_{\rm eq},\mu_{\rm eq}) = -\mathcal{C}_O\,(\Delta_L+\Delta_R)\int d\omega\,\frac{\partial A(\omega)}{\partial \epsilon_d} \times\left\{ f_{T_{\rm eq},\mu_{\rm eq}}(\omega) - \frac{\Delta_L f_{T_L,\mu_L}(\omega) + \Delta_R f_{T_R,\mu_R}(\omega)}{\Delta_L+\Delta_R}\right\}. \quad (19)$$

By comparing Eqs. (18) and (19), we immediately recognize that

$$O_0(T_L,\mu_L,T_R,\mu_R) = O_0(T^*,\mu^*,T^*,\mu^*), \quad (20)$$

provided that

$$\left.\frac{\delta O_p(T_p,\mu_p)}{\Delta_p}\right|_{T_p=T^*,\,\mu_p=\mu^*,\,\Delta_p\to 0} = 0 \quad (21)$$

can be achieved. In relation to Eq. (3b), Eq. (21) further requires that the perturbation to the local observable O by the coupled probe minimizes to zero.

Equation (20) is the central result of this work. As illustrated in Fig. 1, it establishes a quantitative relation between the local property of a nonequilibrium dot and that of a reference equilibrium dot. The physical significance of T^* is thus clarified: The electronic excitations induced by a bias voltage or temperature gradient can be equivalently characterized as thermal excitations induced by a uniform equilibrium temperature. This then provides a *microscopic* interpretation of the MPC-based definition of local temperature.

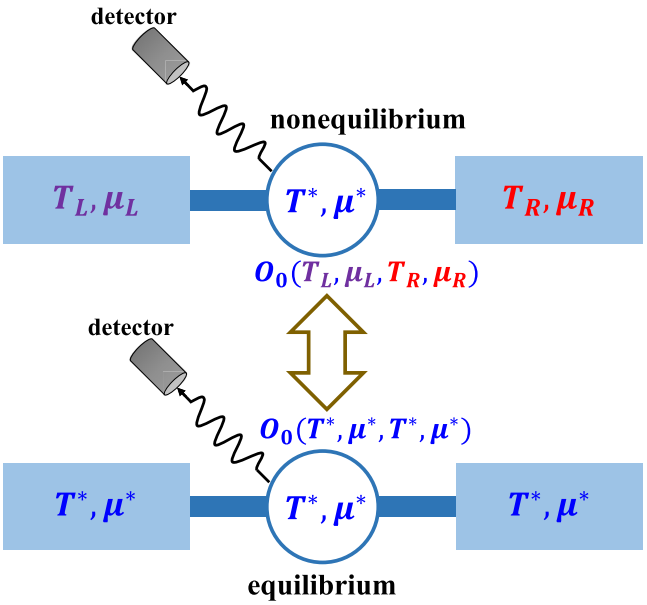

FIG. 1. Schematic illustration of Eq. (20). The local observable O_0 of a nonequilibrium QD can be made equivalent to that of a reference equilibrium QD, provided the two dots have the same local temperature T^*.

It is worth emphasizing that the approximation of Eq. (4) for μ^* does not invalidate the quantitative relation of Eq. (20). This is because μ^* appears only in the Fermi function during the derivation of Eq. (20), and thus the specific form or value of μ^* has no effect on the equality in Eq. (20).

In contrast, within the same conditions, the ZCC of Eqs. (1a) and (1b) amounts to

$$\int d\omega\,(\omega-\mu^*)^k\,A(\omega) \times\left\{ f_{T^*,\mu^*}(\omega) - \frac{\Delta_L f_{T_L,\mu_L}(\omega) + \Delta_R f_{T_R,\mu_R}(\omega)}{\Delta_L+\Delta_R}\right\} = 0. \quad (22)$$

The integral in Eq. (22) has a distinctly different form from that in Eq. (19), suggesting that in general the local temperature T^* determined by the ZCC does not guarantee the equality in Eq. (20).

2. *The case of finite bandwidth*

For leads with a finite bandwidth, $A_s(\omega)$ depends explicitly on the lead chemical potential μ_α. Consequently, the nonequilibrium dot spectral function $A_0(\omega;\mu_L,\mu_R)$ differs from the equilibrium counterpart $A_0(\omega;\mu_{\rm eq},\mu_{\rm eq})$. Nevertheless, as will be shown below, the correspondence relation of Eq. (20) still holds under a small applied bias voltage $V=\mu_R-\mu_L$.

From Eq. (4), we have $\mu_L=\mu^*-\zeta_R V$ and $\mu_R=\mu^*+\zeta_L V$. Define $\eta(\omega;\mu^*)\equiv W^2/[(\omega-\mu^*)^2+W^2]$, and $\eta_\alpha(\omega)$ can be expanded as

$$\eta_L(\omega) = \eta(\omega;\mu^*) - 2\zeta_R\left[\frac{\eta(\omega;\mu^*)}{W}\right]^2(\omega-\mu^*)V + \mathcal{O}(V^2), \quad (23)$$

$$\eta_R(\omega) = \eta(\omega;\mu^*) + 2\zeta_L\left[\frac{\eta(\omega;\mu^*)}{W}\right]^2(\omega-\mu^*)V + \mathcal{O}(V^2). \quad (24)$$

We thus have

$$\Delta_L\,\eta_L(\omega) + \Delta_R\,\eta_R(\omega) = (\Delta_L+\Delta_R)\,\eta(\omega;\mu^*) + \mathcal{O}(V^2). \quad (25)$$

This leads to the equality of

$$A_0(\omega;\mu_L,\mu_R) = A_0(\omega;\mu^*,\mu^*) + \mathcal{O}(V^2). \quad (26)$$

The perturbation to local observable O can thus be expressed as

$$\left.\frac{\delta O_p(T_p,\mu_p)}{\Delta_p}\right|_{T_p=T^*,\,\mu_p=\mu^*,\,\Delta_p\to 0} = -\mathcal{C}_O \int d\omega \,\frac{\partial A_0(\omega)}{\partial \epsilon_d}\left\{ f_{T^*,\mu^*}(\omega) - \frac{\zeta_L\,\eta_L(\omega) f_{T_L,\mu_L}(\omega) + \zeta_R\,\eta_R(\omega) f_{T_R,\mu_R}(\omega)}{\zeta_L\,\eta_L(\omega) + \zeta_R\,\eta_R(\omega)}\right\} + \mathcal{O}(V^2). \tag{27}$$

Substituting Eqs. (25) and (26) into Eq. (15) leads to

$$O_0(T_L,\mu_L,T_R,\mu_R) - O_0(T^*,\mu^*,T^*,\mu^*) = -\mathcal{C}_O(\Delta_L+\Delta_R)\int d\omega\,\frac{\partial A_0(\omega)}{\partial \epsilon_d} \times\left\{ f_{T^*,\mu^*}(\omega) - \frac{\zeta_L\,\eta_L(\omega) f_{T_L,\mu_L}(\omega) + \zeta_R\,\eta_R(\omega) f_{T_R,\mu_R}(\omega)}{\zeta_L\,\eta_L(\omega) + \zeta_R\,\eta_R(\omega)}\right\} + \mathcal{O}(V^2). \tag{28}$$

By comparing Eqs. (27) and (28), one easily recognizes that

$$O_0(T_L,\mu_L,T_R,\mu_R) = O_0(T^*,\mu^*,T^*,\mu^*) + \mathcal{O}(V^2), \tag{29}$$

provided the zero perturbation of Eq. (27) is reached.

C. Interacting dots

For QDs with a finite U, the e-e interacting self-energies [$\Sigma^r_{\rm ee}(\omega)$ and $\Sigma^<_{\rm ee}(\omega)$] depend explicitly on system parameters such as Coulomb energy U, dot level ϵ_d, temperature T_α, and chemical potential μ_α, and thus usually assume a complicated form. This makes an analytical analysis rather difficult. Therefore, the correspondence relation for interacting QDs is to be verified numerically by employing the accurate hierarchical equations of motion (HEOM) approach, as described in the following Sec. III D.

D. Hierarchical equations of motion approach for quantum impurity systems

To verify the above analytical analysis, and to demonstrate that Eq. (20) underscores the physical significance of T^*, we perform numerical calculations on the QD systems with an accurate and universal HEOM approach [53–59]. The detailed derivation of the HEOM formalism has been presented in Refs. [53,55]. The HEOM theory is formally rigorous, and the numerical approach has been routinely used to investigate the equilibrium and nonequilibrium properties of strongly-correlated quantum impurity systems [60–68].

The numerical results of the HEOM method are guaranteed to be quantitatively accurate provided they converge with respect to the truncation level of the hierarchy $N_{\rm trun}$. For the noninteracting (interacting) QDs studied in this work, the convergence is achieved at $N_{\rm trun} = 2$ (4), unless otherwise specified.

IV. NUMERICAL ANALYSIS AND DISCUSSIONS

Figure 2(a) shows T^* determined by the MPC and the ZCC for a noninteracting QD of varying ϵ_d under a fixed bias voltage. The ZCC predicts an almost constant T^* over a large range of ϵ_d. In contrast, the MPC results in a conspicuous fluctuation of T^* around $\epsilon_d = -0.7\Delta$ ($\Delta = \Delta_L + \Delta_R$ is taken as the unit of energy), where the magnitude of T^* deviates significantly from the ZCC value. The vertical lines in Fig. 2(a) enclose a region (region II) in which the MPC-determined T^* varies sharply with increasing ϵ_d. In this region the zero-perturbation condition, Eq. (21), is out of reach no matter how T_p is varied, while in the other regions (I and III) Eq. (21) is satisfied for any ϵ_d, as exemplified in Fig. 2(d).

We now examine the correspondence relation for local properties, which is cast in a simplified form of $O_0(T,V) = O_0(T^*,0)$ in the case $T_L = T_R = T$. Figure 2(b) shows the relative deviation $[\chi_0^m(T^*,0) - \chi_0^m(T,V)]/\chi_0^m(T,V)$ obtained numerically. With T^* determined by the MPC, such deviation appears to be vanishingly small in regions I and III, where the zero-perturbation condition, Eq. (21), is always achievable; while in region II the deviation remains appreciable. This clearly verifies our analytical conclusion that the zero perturbation condition for determining T^* is a prerequisite for the correspondence relation to hold. In contrast, with T^* determined by the ZCC, the correspondence relation does not apply over the large range of ϵ_d examined.

The existence of the three distinct regions for the MPC-determined T^* can be understood as follows. As shown in Fig. 2(c), the dot spectral function $A(\omega)$ exhibits a single peak

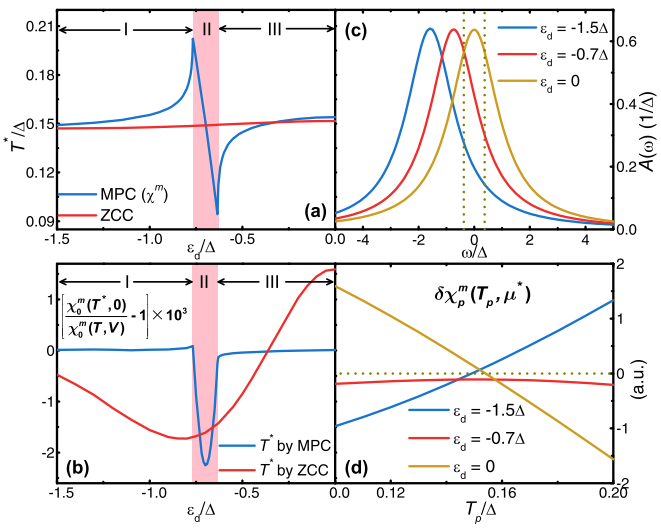

FIG. 2. Calculated (a) T^* and (b) relative deviation between $\chi_0^m(T,V)$ and $\chi_0^m(T^*,0)$ versus ϵ_d for a noninteracting QD under a bias voltage V. (c) Dot spectral function $A(\omega)$ and (d) $\delta\chi_p^m$ versus T_p for different ϵ_d. The QD parameters are (in units of Δ): $U = 0$, $T_L = T_R = T = 0.1$, $\mu_R = -\mu_L = V/2 = 0.2$, $\Delta_L = \Delta_R = 0.5$, $\Omega_L = \Omega_R = 0$, and $W_L = W_R = 20$. The vertical lines and regions are explained in the main text.

centered at ϵ_d and broadened by Δ. Under a finite voltage, most of the electronic excitations occur within an energy window $(\mu_L - \omega_L, \mu_R + \omega_R)$, where ω_α is the full width at half maximum of $\frac{\partial}{\partial\omega} f_{T_\alpha,\mu_\alpha}(\omega)$. For a dot in region I (such as $\epsilon_d = -1.5\Delta$), the bulk of the dot spectral peak lies below the excitation window, and the dot level is off-resonant with the lead states. Consequently, the electronic excitations are largely local on the dot, and the MPC-determined T^* precisely captures the magnitudes of these local excitations.

In contrast, for a dot in region III (such as $\epsilon_d = 0$), the center of the dot spectral peak resides precisely in the excitation window, indicating that the dot level is in strong resonance with the lead states. Therefore, excitations occur mostly inside the leads to create hot electrons (holes) above (below) the Fermi energy and hence are rather *nonlocal*. In such a case, the MPC-determined T^* quantifies the magnitude of these nonlocal excitations. In this respect, it is more appropriate to interpret T^* as an "effective temperature" rather than a local temperature.

Finally, for a dot in region II (such as $\epsilon_d = -0.7\Delta$), the spectral peak lies at the edge of the excitation window. The dot is thus in a near-resonance situation, and local and nonlocal excitations could both take place. Since the local and nonlocal excitations are intrinsically different, their influence on the local properties cannot be adequately addressed by a single thermodynamic parameter T^*. This thus explains why the zero-perturbation condition of Eq. (21) is out of reach in region II.

Analytical analysis is somewhat difficult for interacting QDs, and therefore we resort to a numerical analysis by employing the HEOM approach. For a QD with $U > 0$, the local observables $\chi^m = -\frac{1}{2}g^2\mu_B^2(\frac{\partial\langle n_\uparrow\rangle}{\partial\epsilon_\uparrow} - \frac{\partial\langle n_\downarrow\rangle}{\partial\epsilon_\uparrow})$ and $\chi^c = -2(\frac{\partial\langle n_\uparrow\rangle}{\partial\epsilon_\uparrow} + \frac{\partial\langle n_\downarrow\rangle}{\partial\epsilon_\uparrow})$ are nonequivalent because $\frac{\partial\langle n_\downarrow\rangle}{\partial\epsilon_\uparrow} \neq 0$. Therefore, the MPC-determined local temperature depends on the specific choice of local observable O. Nevertheless, our calculations have shown that over a wide range of parameters the use of χ^m and χ^c result in very close values of T^* (see Fig. 3).

As it has been pointed out in Sec. II B, in principle, the MPC can be imposed directly on the system reduced density matrix ρ, and the determined T^* would truly reflect the change of system state and be independent of any observable. However, in practice, it is difficult to monitor the change of ρ, and we have to choose a physical observable so that the MPC-based definition could become experimentally realizable.

Figures 3(a) and 3(b) depict the variation of T^* with increasing U at a high $(T = \Delta)$ and low $(T = 0.1\Delta)$ background temperature, respectively. Similar to the noninteracting situation, the ZCC predicts an almost constant T^* over a large range of U, while the MPC again gives rise to a sharp transition of T^* within a small region (region II) of U. The relative deviations $[O_0(T^*,0) - O_0(T,V)]/O_0(T,V)$ ($O = \chi^m$ and χ^c) are shown in Figs. 3(c) and 3(d). While the ZCC-defined T^* does not conform to the correspondence relation of Eq. (20), the MPC-determined T^* leads to rather minor deviations so long as the zero perturbation of Eq. (21) can be achieved (in regions I and III). Here, the regions I, II, and III correspond to the off-resonant, near-resonant, and resonant situations, respectively, as supported by the positions

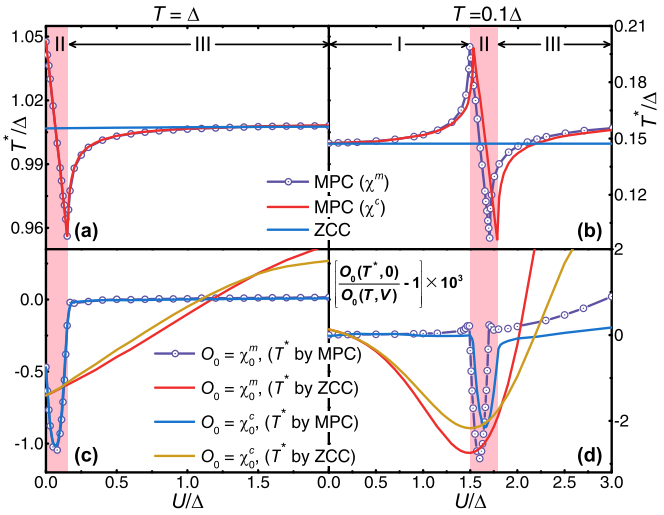

FIG. 3. Calculated T^* versus U for an interacting QD under a bias voltage V at the background temperature (a) $T = \Delta$ and (b) $T = 0.1\Delta$. The relative deviations between $O_0(T,V)$ and $O_0(T^*,0)$ are shown in (c) and (d), respectively. The QD parameters are (in units of Δ): $\epsilon_d = -2$, $\mu_R = -\mu_L = V/2 = 0.2$, $\Delta_L = \Delta_R = 0.5$, $\Omega_L = \Omega_R = 0$, and $W_L = W_R = 20$. The vertical lines and regions are explained in the main text.

of the dot spectral peaks with respect to the excitation energy window.

Figure 4 depicts the HEOM calculated dot spectral functions of interacting QDs with different values of U. As shown in Fig. 4(a), at a relatively higher background temperature $(T = \Delta)$ the renormalized Hubbard peak gradually moves into the excitation energy window with the increase of U. For instance, for the QD with $U = 1.5\Delta$ the renormalized Hubbard peak resides largely within the excitation window, and hence the QD is in a resonant situation.

At a low background temperature (such as $T = 0.1\Delta$) the deviation between $\chi_0^m(T,V)$ and $\chi_0^m(T^*,0)$ (with the MPC-determined T^*) assumes a small but finite value in region III; see Fig. 3(d). This is because Kondo resonant states start to emerge as U increases. As shown in Fig. 4(b), for the QD with $U = 5\Delta$ a prominent Kondo spectral peak forms at the center of the excitation energy window. The presence of Kondo resonance states is clearly demonstrated by the inset

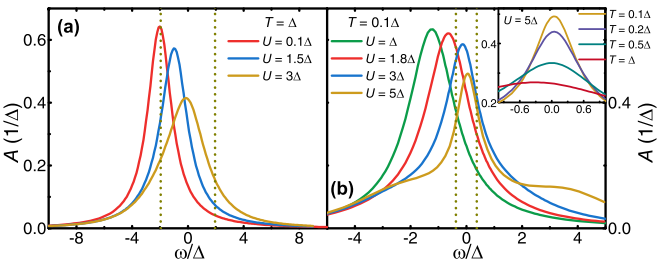

FIG. 4. Dot spectral function $A(\omega)$ of a nonequilibrium QD with a varying of U at the background temperature (a) $T = \Delta$ and (b) $T = 0.1\Delta$. The inset of (b) shows the Kondo spectral peak at various T. The vertical lines mark the excitation energy window $(\mu_L - \omega_L, \mu_R + \omega_R)$. The QD parameters are the same as in the caption of Fig. 3.

of Fig. 4(b), in which the peak height increases continuously with the lowering of temperature. Under a bias voltage, Kondo resonant states facilitate electron co-tunneling processes, which can be understood as the concurrence of local spin-flip and nonlocal electron-transfer excitations. As in the case of noninteracting electrons, such mixed-ranged excitations cannot be fully captured by the single parameter T^*, and hence the correspondence relation for local observables does not hold.

V. CONCLUDING REMARKS

Based on the above analysis, we can now answer the question of how to physically interpret the defined or measured local temperature. The ZCC-based definition does give a T^* that is higher than the background T, indicating the presence of local heating. However, the magnitude of T^* can hardly be associated with the changes in system local observables. In contrast, the MPC-based definition establishes a quantitative correspondence between the nonequilibrium system of interest and a reference equilibrium system. The correspondence relation holds as long as the following three conditions are met: (i) the perturbation induced by the probe minimizes to zero, (ii) the monitored observable is a local property, and (iii) the electronic excitations driven by the external source are fully local.

Finally, from the experimental perspective the MPC-based definition is obviously more practical, as it does not require measuring the heat currents directly. Even if the zero perturbation to a local observable is out of reach, the MPC of Eq. (3b) always provides a definitive measurement for the magnitude of T^*. In fact, the nonzero minimal perturbation indicates the presence of a nonlocal contribution to local heating from electronic excitations in the environment. In view of the fact that local thermal probes as those suggested in this work are now being developed, we hope our studies will provide a firmer basis for understanding the ensuing quantities they measure.

ACKNOWLEDGMENTS

The support from the Ministry of Science and Technology of China (Grants No. 2016YFA0400900 and No. 2016YFA0200600), the National Natural Science Foundation of China (Grants No. 21233007, No. 21322305, No. 21573202, and No. 21633006), the Fundamental Research Funds for Chinese Central Universities (Grants No. 2030020028 and No. 2340000074), and the Strategic Priority Research Program (B) of the Chinese Academy of Sciences (Grant No. XDB01020000) is gratefully appreciated. M.D.V. acknowledges support from Department of Energy under Grant No. DE-FG02-05ER46204.

[1] G. Schulze, K. J. Franke, A. Gagliardi, G. Romano, C. S. Lin, A. L. Rosa, T. A. Niehaus, T. Frauenheim, A. Di Carlo, A. Pecchia, and J. I. Pascual, Phys. Rev. Lett. **100**, 136801 (2008).
[2] E. A. Hoffmann, H. A. Nilsson, J. E. Matthews, N. Nakpathomkun, A. I. Persson, L. Samuelson, and H. Linke, Nano Lett. **9**, 779 (2009).
[3] S. Berciaud, M. Y. Han, K. F. Mak, L. E. Brus, P. Kim, and T. F. Heinz, Phys. Rev. Lett. **104**, 227401 (2010).
[4] K. L. Grosse, M.-H. Bae, F. Lian, E. Pop, and W. P. King, Nat. Nanotechnol. **6**, 287 (2011).
[5] F. Menges, P. Mensch, H. Schmid, H. Riel, A. Stemmer, and B. Gotsmann, Nat. Commun. **7**, 10874 (2016).
[6] D. Mann, Y. K. Kato, A. Kinkhabwala, E. Pop, J. Cao, X. Wang, L. Zhang, Q. Wang, J. Guo, and H. Dai, Nat. Nanotechnol. **2**, 33 (2007).
[7] C. Y. Jin, Z. Li, R. S. Williams, K.-C. Lee, and I. Park, Nano Lett. **11**, 4818 (2011).
[8] W. Lee, K. Kim, W. Jeong, L. A. Zotti, F. Pauly, J. C. Cuevas, and P. Reddy, Nature (London) **498**, 209 (2013).
[9] J.-M. Yang, H. Yang, and L. Lin, ACS nano **5**, 5067 (2011).
[10] J. S. Donner, S. A. Thompson, M. P. Kreuzer, G. Baffou, and R. Quidant, Nano Lett. **12**, 2107 (2012).
[11] G. Ke, C. Wang, Y. Ge, N. Zheng, Z. Zhu, and C. J. Yang, J. Am. Chem. Soc. **134**, 18908 (2012).
[12] G. Kucsko, P. C. Maurer, N. Y. Yao, M. Kubo, H. J. Noh, P. K. Lo, H. Park, and M. D. Lukin, Nature (London) **500**, 54 (2013).
[13] Y.-C. Chen, M. Zwolak, and M. Di Ventra, Nano Lett. **3**, 1691 (2003).
[14] M. Di Ventra, *Electrical Transport in Nanoscale Systems* (Cambridge University Press, 2008).
[15] Z. Huang, F. Chen, R. D'Agosta, P. A. Bennett, M. D. Ventra, and N. Tao, Nat. Nanotechnol. **2**, 698 (2007).
[16] Y. Dubi and M. Di Ventra, Rev. Mod. Phys. **83**, 131 (2011).
[17] J. P. Heremans, M. S. Dresselhaus, L. E. Bell, and D. T. Morelli, Nat. Nanotechnol. **8**, 471 (2013).
[18] H. Thierschmann, R. Sánchez, B. Sothmann, F. Arnold, C. Heyn, W. Hansen, H. Buhmann, and L. W. Molenkamp, Nat. Nanotechnol. **10**, 854 (2015).
[19] Y. Kim, W. Jeong, K. Kim, W. Lee, and P. Reddy, Nat. Nanotechnol. **9**, 881 (2014).
[20] D. Rakhmilevitch, R. Korytár, A. Bagrets, F. Evers, and O. Tal, Phys. Rev. Lett. **113**, 236603 (2014).
[21] C. N. Raju and A. Chatterjee, Sci. Rep. **6**, 18511 (2016).
[22] Z. Huang, B. Xu, Y. Chen, M. Di Ventra, and N. Tao, Nano Lett. **6**, 1240 (2006).
[23] M. Tsutsui, M. Taniguchi, and T. Kawai, Nano Lett. **8**, 3293 (2008).
[24] Z. Ioffe, T. Shamai, A. Ophir, G. Noy, I. Yutsis, K. Kfir, O. Cheshnovsky, and Y. Selzer, Nat. Nanotechnol. **3**, 727 (2008).
[25] D. R. Ward, D. A. Corley, J. M. Tour, and D. Natelson, Nat. Nanotechnol. **6**, 33 (2011).
[26] M. Tsutsui, T. Morikawa, A. Arima, and M. Taniguchi, Sci. Rep. **3**, 3326 (2013).
[27] R. Chen, P. J. Wheeler, M. Di Ventra, and D. Natelson, Sci. Rep. **4**, 4221 (2014).
[28] E. Tikhonov, D. Shovkun, D. Ercolani, F. Rossella, M. Rocci, L. Sorba, S. Roddaro, and V. Khrapai, Sci. Rep. **6**, 30621 (2016).
[29] M. Hartmann, G. Mahler, and O. Hess, Phys. Rev. Lett. **93**, 080402 (2004).

[30] J. P. Pekola, T. T. Heikkilä, A. M. Savin, J. T. Flyktman, F. Giazotto, and F. W. J. Hekking, Phys. Rev. Lett. **92**, 056804 (2004).
[31] M. Galperin, A. Nitzan, and M. A. Ratner, Phys. Rev. B **75**, 155312 (2007).
[32] Y. Dubi and M. Di Ventra, Nano Lett. **9**, 97 (2009).
[33] M. Di Ventra and Y. Dubi, Europhys. Lett. **85**, 40004 (2009).
[34] A. Caso, L. Arrachea, and G. S. Lozano, Phys. Rev. B **83**, 165419 (2011).
[35] P. Ribeiro, F. Zamani, and S. Kirchner, Phys. Rev. Lett. **115**, 220602 (2015).
[36] J. P. Bergfield, S. M. Story, R. C. Stafford, and C. A. Stafford, ACS nano **7**, 4429 (2013).
[37] J. Meair, J. P. Bergfield, C. A. Stafford, and P. Jacquod, Phys. Rev. B **90**, 035407 (2014).
[38] J. P. Bergfield, M. A. Ratner, C. A. Stafford, and M. Di Ventra, Phys. Rev. B **91**, 125407 (2015).
[39] L. Z. Ye, D. Hou, X. Zheng, Y. J. Yan, and M. Di Ventra, Phys. Rev. B **91**, 205106 (2015).
[40] F. G. Eich, M. Di Ventra, and G. Vignale, Phys. Rev. B **93**, 134309 (2016).
[41] F. G. Eich, A. Principi, M. Di Ventra, and G. Vignale, Phys. Rev. B **90**, 115116 (2014).
[42] H.-L. Engquist and P. W. Anderson, Phys. Rev. B **24**, 1151 (1981).
[43] D. Sánchez and L. Serra, Phys. Rev. B **84**, 201307 (2011).
[44] P. A. Jacquet and C.-A. Pillet, Phys. Rev. B **85**, 125120 (2012).
[45] J. P. Bergfield and C. A. Stafford, Phys. Rev. B **90**, 235438 (2014).
[46] A. Shastry and C. A. Stafford, Phys. Rev. B **92**, 245417 (2015).
[47] C. A. Stafford, Phys. Rev. B **93**, 245403 (2016).
[48] P. W. Anderson, Phys. Rev. **124**, 41 (1961).
[49] A.-P. Jauho, N. S. Wingreen, and Y. Meir, Phys. Rev. B **50**, 5528 (1994).
[50] J. P. Bergfield and C. A. Stafford, Phys. Rev. B **79**, 245125 (2009).
[51] Y. Meir and N. S. Wingreen, Phys. Rev. Lett. **68**, 2512 (1992).
[52] B. Dong and X. L. Lei, J. Phys. Condens. Matter **14**, 11747 (2002).
[53] J. S. Jin, X. Zheng, and Y. J. Yan, J. Chem. Phys. **128**, 234703 (2008).
[54] X. Zheng, J. S. Jin, S. Welack, M. Luo, and Y. J. Yan, J. Chem. Phys. **130**, 164708 (2009).
[55] Z. H. Li, N. H. Tong, X. Zheng, D. Hou, J. H. Wei, J. Hu, and Y. J. Yan, Phys. Rev. Lett. **109**, 266403 (2012).
[56] R. Härtle, G. Cohen, D. R. Reichman, and A. J. Millis, Phys. Rev. B **88**, 235426 (2013).
[57] R. Härtle and A. J. Millis, Phys. Rev. B **90**, 245426 (2014).
[58] R. Härtle, G. Cohen, D. R. Reichman, and A. J. Millis, Phys. Rev. B **92**, 085430 (2015).
[59] S. Wenderoth, J. Bätge, and R. Härtle, Phys. Rev. B **94**, 121303 (2016).
[60] X. Zheng, Y. J. Yan, and M. Di Ventra, Phys. Rev. Lett. **111**, 086601 (2013).
[61] L. Z. Ye, D. Hou, R. Wang, D. Cao, X. Zheng, and Y. J. Yan, Phys. Rev. B **90**, 165116 (2014).
[62] D. Hou, R. Wang, X. Zheng, N. H. Tong, J. H. Wei, and Y. J. Yan, Phys. Rev. B **90**, 045141 (2014).
[63] Y. Wang, X. Zheng, B. Li, and J. Yang, J. Chem. Phys. **141**, 084713 (2014).
[64] D. Hou, S. Wang, R. Wang, L. Ye, R. Xu, X. Zheng, and Y. Yan, J. Chem. Phys. **142**, 104112 (2015).
[65] X. Wang, D. Hou, X. Zheng, and Y. Yan, J. Chem. Phys. **144**, 034101 (2016).
[66] Y. Wang, X. Zheng, and J. Yang, Phys. Rev. B **93**, 125114 (2016).
[67] L. Ye, X. Wang, D. Hou, R.-X. Xu, X. Zheng, and Y. Yan, WIREs Comput. Mol. Sci. **6**, 608 (2016).
[68] Y. Wang, X. Zheng, and J. Yang, J. Chem. Phys. **145**, 154301 (2016).